

CrossMark
click for updatesCite this: *RSC Adv.*, 2014, 4, 36713Received 17th June 2014
Accepted 7th August 2014

DOI: 10.1039/c4ra05833j

www.rsc.org/advances

Synthesis, characterization and catalytic activity of graphene oxide/ZnO nanocomposites

Mahmoud Nasrollahzadeh,^{*a} Babak Jaleh^b and Ameneh Jabbari^b

This paper reports on the synthesis and use of graphene oxide/ZnO nanocomposite as a heterogeneous catalyst for the synthesis of various tetrazoles. The catalyst was characterized by X-ray diffraction (XRD), scanning electron microscopy (SEM), energy dispersive X-ray spectroscopy (EDS), transmission electron microscopy (TEM) and UV-vis spectroscopy. This method has the advantages of high yields, elimination of homogeneous catalysts or corrosive acids, simple methodology and easy work up. Another important factor is the stability and recyclability of the catalyst under the reaction conditions used. This heterogeneous catalyst shows no significant loss of activity in the recycling experiments.

Introduction

The importance of tetrazole chemistry, especially for applications in coordination and medicinal chemistry, organic synthesis and materials applications has led to significant research by organic chemist researchers.¹

Tetrazoles are conventionally synthesized *via* reaction of dangerous and harmful hydrazoic acid or azide ions with nitriles, thiocyanates or cyanamides in the presence of homogeneous catalysts.^{1,2} Earlier reported methods for the synthesis of tetrazoles suffered from drawbacks such as the use of expensive, toxic and moisture sensitive reagents and stoichiometric amounts of homogeneous catalysts, environmental pollution caused by formation of heavy metal waste, low yields, harsh reaction conditions, the poor availability or difficulty in preparing the starting materials or catalysts, tedious work-ups, and environmental pollution caused by the formation of side products. As a result, these drawbacks have limited tetrazoles large scale applications in industry. Later tetrazoles were prepared from the reaction between thiocyanates or nitriles with NaN₃ and NH₄Cl as a substitute for HN₃.³ However, combining sodium azide with ammonium chloride as an acid may yield gaseous HN₃, which is potentially dangerous and toxic. Therefore, the need for improved methods that reduce or eliminate the use and generation of hazardous compounds is essential.

In addition, several syntheses of tetrazoles have been reported in the presence of homogeneous catalysts, while less expensive heterogeneous catalysts have less received attention. The problem with homogeneous catalysis is the difficulty to

separate the catalyst from the reaction mixture and the impossibility of reuse it in consecutive reactions. Moreover, with by using inexpensive and noncorrosive heterogeneous catalysts, chemical transformations occur, especially for industrial processes, with higher efficiency and give better purities of the products, and offer easier work-up, which create economic and ecological advantages. Thus, due to safety considerations, it is desirable to develop a more efficient and convenient method for the synthesis of tetrazoles under heterogeneous conditions.

Recently, a newly layered material-graphene oxide (GO) has attracted much attention of scientists all over the world, since it exhibits unique surface properties (oxygenated functional groups on the basal planes and edge), high-specific surface area, and easy exfoliation into monolayers under water.⁴ Graphene oxide, a delaminated layer of graphite oxide is shown in Fig. 1. GO consists of intact graphitic regions interspersed with sp³-hybridized carbons containing carboxyl, hydroxyl, and epoxide functional groups on the edge, top, and bottom surface of each sheet and sp²-hybridized carbons on the aromatic network.⁵ In addition, due to its low-cost, thermal, chemical and mechanical stability, large specific surface area and strong interactions with metal clusters, GO is a promising material for catalytic applications.⁶ The dispersion of metal oxide or metal nanoparticles on GO potentially provides a new way to develop catalytic materials.⁶ However, only a few metal oxide or metal nanoparticles-graphene (or graphene oxide) hybrids have been reported and fewer studies have investigated their catalytic properties.⁷ We recently published synthesis of copper nanoparticles supported on reduced graphene oxide as a highly active and recyclable catalyst for the preparation of formamides and primary amines.⁸

In continuation of our researches on the synthesis of tetrazoles and application of heterogeneous catalysts,^{1,9} we report a new protocol for the preparation of the graphene oxide/ZnO

^aDepartment of Chemistry, Faculty of Science, University of Qom, Qom 37185-369, Iran. E-mail: mahmoudnasr81@gmail.com; Fax: +98 25 32103595; Tel: +98 25 32850953

^bDepartment of Physics, Bu-Ali Sina University, Postal Code 65174, Hamedan, Iran

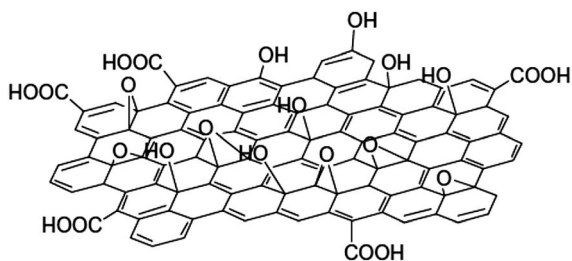
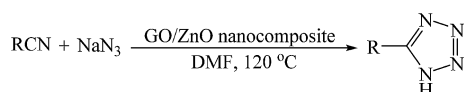


Fig. 1 Proposed structure of graphene oxide (GO).



Scheme 1 Formation of 5-substituted-1H-tetrazoles using GO/ZnO nanocomposite.

nanocomposite and its catalytic applications as a novel and stable heterogeneous catalyst for the synthesis of 5-substituted-1H-tetrazoles (Scheme 1). Environmental acceptability, economic viability, and recyclability of the graphene oxide/ZnO nanocomposite are the advantages of this novel catalyst.

Result and discussion

An advantage of the graphene oxide/ZnO nanocomposite catalyst was that its synthesis was very simple.

Characterization of catalyst

The catalyst was characterized using the powder XRD, SEM, EDS, TEM and UV-vis spectroscopy.

We used energy dispersive X-ray spectroscopy (EDS) to determine chemical composition of GO/ZnO (Fig. 2). In the EDS spectrum of catalyst, peaks related to C, O and Zn were observed. The atomic and weight ratios are listed in Table 1.

Fig. 3 shows the XRD patterns of the as-prepared GO/ZnO nanocomposite. GO exhibit a (002) broad diffraction peak at

Table 1 EDS data of graphene oxide/ZnO

Element	Series	Norm. C [wt%]	Atom. C [at%]
Carbon	K series	24.70	47.80
Oxygen	K series	23.20	33.69
Zinc	K series	52.10	18.51

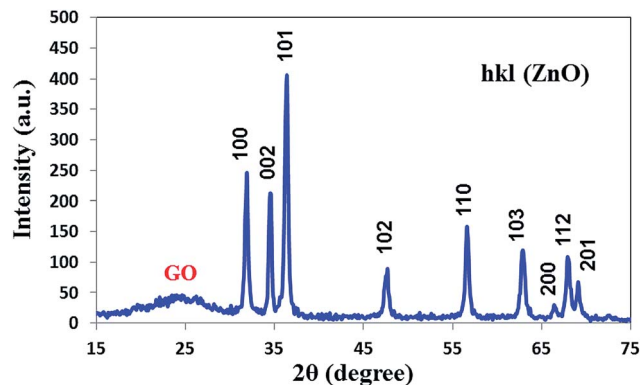


Fig. 3 XRD pattern of GO/ZnO nanocomposite.

26.1°. Also the other diffraction peaks of GO/ZnO nanocomposite are similar to that of pure ZnO and correspond to the hexagonal phase of ZnO (JPCDS 36-1451).

According to the XRD data, the mean crystalline size (D) of the ZnO nanoparticles in graphene oxide/ZnO sample was calculated by using the Debye Scherrer formula:^{10b}

$$D = \frac{0.9\lambda}{\beta \cos \theta} \quad (1)$$

where $\lambda = 1.54 \text{ \AA}$ is the wavelength of the X-ray radiation used, θ is the Bragg diffraction angle of the XRD peak and β is the measured broadening of the diffraction line peak at the angle of 2θ , at half its maximum intensity (FWHM) in radian. As mentioned, ZnO has hexagonal unit cell with two lattice parameters ('a' and 'c') which can be estimated from the XRD data by using the following equations:^{10b}

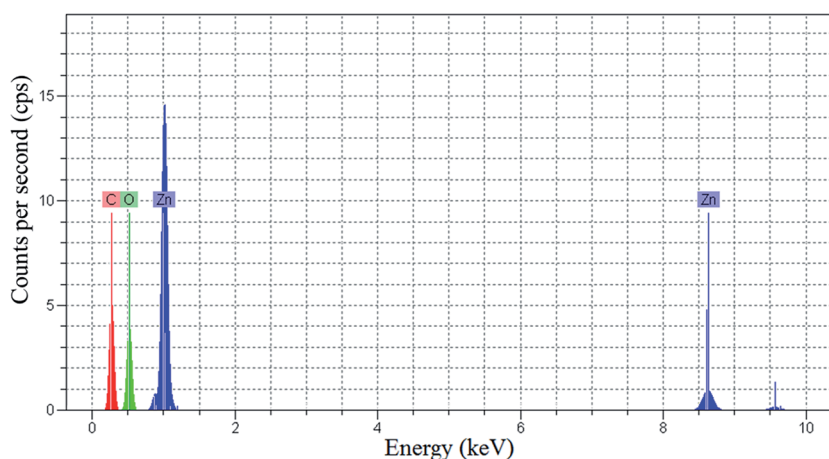


Fig. 2 EDS spectrum of graphene oxide/ZnO.

$$d_{hkl} = \frac{1}{\sqrt{4(h^2 + k^2 + hk)/3a^2 + l^2/c^2}} \quad (2)$$

$$a = \frac{\lambda}{\sqrt{3}\sin\theta_{100}}, \quad c = \frac{\lambda}{\sin\theta_{002}} \quad (3)$$

where d_{hkl} is the inter-planer distance between adjacent planes in the Miller indices (hkl), $\lambda = 1.54 \text{ \AA}$ is the wavelength of the X-ray radiation used, θ_{100} and θ_{002} are the angles of the diffraction peaks (100) and (002) respectively. The lattice parameters for GO/ZnO were calculated from the XRD data by using eqn (2) and (3). The calculated lattice parameters are listed in Table 2.

Table 2 shows that the ZnO particles are nanosized ($D = 19.03 \text{ nm}$). And also d_{hkl} , a and c lattice parameters calculated for GO/ZnO sample are in agreement with pure ZnO (JCPDS 36-1451), which indicates that the presence of GO does not result in the development of new crystal orientations or change in preferential orientations of ZnO. In addition, Fig. 4a–c shows successively the SEM (a and b) and TEM (c) images of GO and GO/ZnO. The light-gray thin films are the GO sheets, and the dark regions on the GO background are due to the presence of ZnO particles. It can be clearly seen in Fig. 4 that the exfoliated GO sheet was decorated with ZnO aggregates with average size of below 30 nm. It is observed that the ZnO particles are nanosized.

A typical UV-vis spectrum of the graphene oxide/ZnO thin films on glass substrates is shown in Fig. 5.

Fig. 6 shows the FT-IR spectra of the pristine GO and GO/ZnO nanocomposite. In the FT-IR spectrum for GO, the broad peak centered at 3431 cm^{-1} is attributed to the O–H stretching vibrations, 1717 cm^{-1} (stretching vibrations from C=O), 1621 cm^{-1} (skeletal vibrations from unoxidized graphitic domains), 1184 cm^{-1} (C–OH stretching vibrations), and at 1050 cm^{-1} (C–O stretching vibrations).^{11a} The broad peak at 3437 cm^{-1} in the FT-IR spectrum of the GO/ZnO nanocomposite might be attributed to the O–H stretching vibration of absorbed water molecules. In addition, the FT-IR spectrum of GO/ZnO shows a peak at 431 cm^{-1} . The band at 451 cm^{-1} corresponds to the E_2 mode of hexagonal ZnO.^{11b}

Activity of graphene oxide/ZnO nanocomposite for the synthesis of 5-substituted-1H-tetrazole

The catalytic behavior of the GO/ZnO nanocomposite was studied for the synthesis of 5-substituted-1H-tetrazole.

Initially, we employed sodium azide and benzonitrile as model substrates for the development of optimized conditions. Control experiments show that there is no reaction in the

Table 2 Some calculated properties of the GO/ZnO nanocomposite

Sample	2θ	hkl	$d_{hkl} (\text{\AA})$	$D (\text{nm})$	Lattice parameters		
					$c (\text{\AA})$	$a (\text{\AA})$	c/a
GO/ZnO	31.900	100	2.29	19.03	5.202	3.248	1.601
	34.500	002	2.601				
JCPDS 36-1451	31.770	100	2.814	—	5.207	3.250	1.602
	34.422	002	2.603				

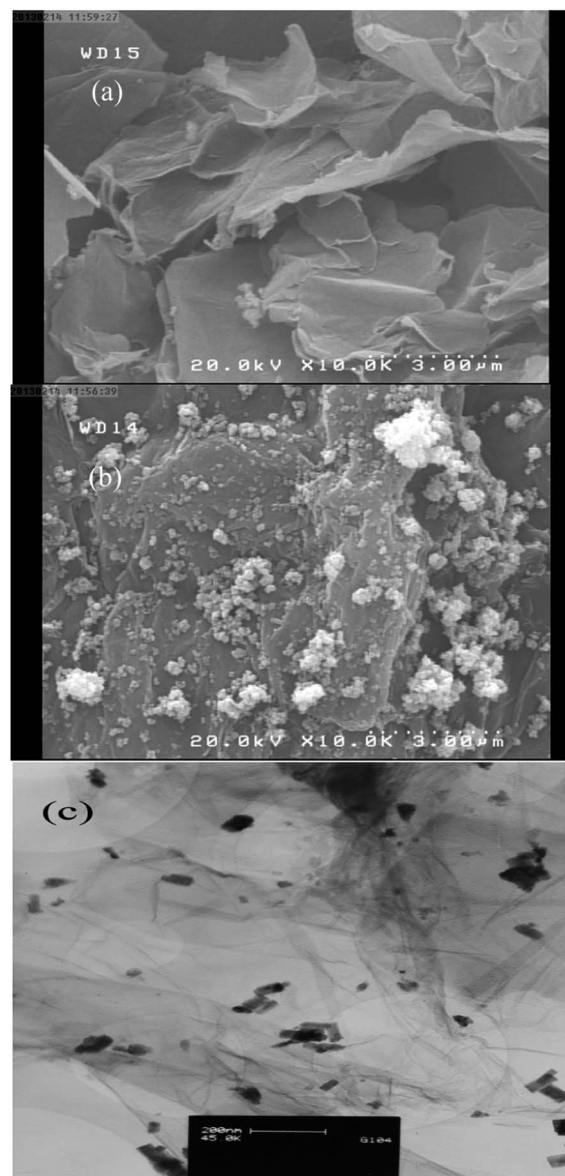


Fig. 4 SEM (a and b) and TEM (c) images of graphene oxide/ZnO nanocomposite.

absence of catalyst (Table 3, entry 11). However, addition of the catalyst to the mixture has rapidly increased the formation of 5-phenyl-1H-tetrazole in high yields. As shown in Table 3, the reaction was influenced significantly by the solvent employed. Among the solvents tested, DMF proved to be the most efficient (Table 3, entry 6). The effect of catalyst loading was probed. Catalyst loads of 0.03 g were typically required to achieve quantitative conversion with most substrates. The use of lower catalyst loadings resulted in incomplete reactions (entry 8). Increasing the amount of catalyst showed no substantial improvement in the yield. We then used the optimal reaction conditions (catalyst (0.03 g), aryl nitrile (2.0 mmol) and sodium azide (3.0 mmol)) for the synthesis of 5-substituted-1H-tetrazoles in DMF ((5.0 mL) at $120 \text{ }^\circ\text{C}$) for the appropriate times and the results are shown in Table 4. Also, to explore the preference

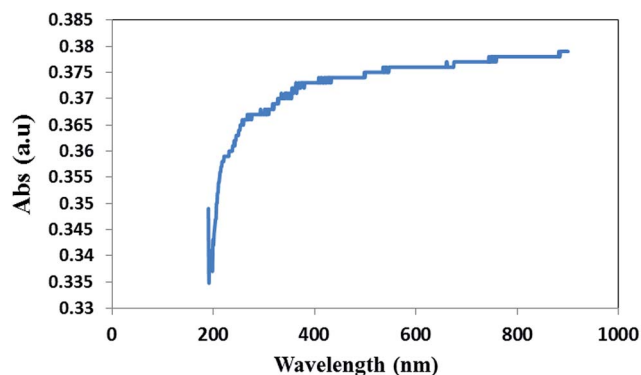


Fig. 5 A typical UV-vis absorption spectrum of the graphene oxide/ZnO thin films on glass substrates.

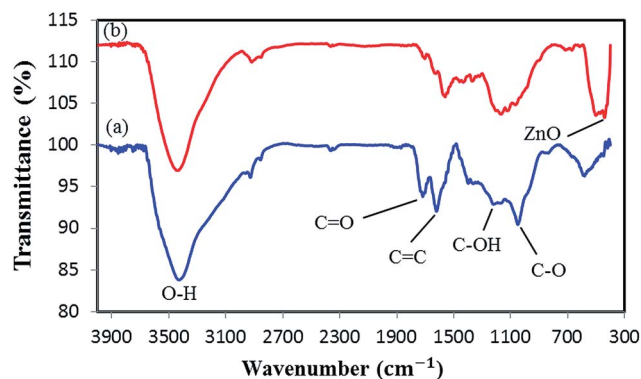


Fig. 6 FTIR spectra of the graphene oxide (a) and GO/ZnO nanocomposite (b).

Table 3 Optimization of reaction conditions in the preparation of 5-phenyl-1*H*-tetrazole^a

Entry	Catalyst (g)	Solvent	Yield ^b (%)
1	GO/ZnO nanocomposite (0.03)	H ₂ O	Trace
2	GO/ZnO nanocomposite (0.03)	MeCN	45
3	GO/ZnO nanocomposite (0.03)	Toluene	46
4	GO/ZnO nanocomposite (0.03)	DMSO	71
5	GO/ZnO nanocomposite (0.03)	NMP	67
6	GO/ZnO nanocomposite (0.03)	DMF	78
7	GO/ZnO nanocomposite (0.05)	DMF	78
8	GO/ZnO nanocomposite (0.01)	DMF	52
9	ZnO (0.04)	DMF	44
10	ZnBr ₂ (0.03)	DMF	68 ^c
11	0.0	DMF	0.0 ^d

^a Reaction conditions: benzonitrile (2.0 mmol), sodium azide (3.0 mmol), catalyst (0.03 g), solvent (5 mL), 120 °C, 30 h. ^b Isolated yield. ^c Stoichiometric amounts are used. ^d In the absence of catalyst at 120 °C, no reaction occurred after 30 h.

of the GO/ZnO nanocomposite over other catalysts such as ZnBr₂ and ZnO, comparison between their catalytic activities was made in the preparation of 5-phenyl-1*H*-tetrazole as the test substrate. As evidenced from Table 3, under comparable conditions in DMF as the solvent, GO/ZnO nanocomposite acts as strong catalyst.

Table 4 Formation of 5-substituted-1*H*-tetrazoles by GO/ZnO nanocomposite^a

$$\text{RCN} + \text{NaN}_3 \xrightarrow[\text{DMF, 120 } ^\circ\text{C}]{\text{GO/ZnO nanocomposite}} \text{R}-\text{C}_5\text{H}_3\text{N}_4$$

Entry	RCN	Product	Yield ^b (%)
1			78
2			82
3			81
4			77
5			80
6			78
7			75
8			67
9			68
10			81
11			71
12			79

^a Reaction conditions: nitrile (2.0 mmol), sodium azide (3.0 mmol), catalyst (0.03 g), DMF (5 mL), 120 °C, 30 h. ^b Yields are after work-up.

Having optimized the conditions, we explored the general applicability of graphene oxide/ZnO nanocomposite as a catalyst for cycloaddition of sodium azide with aryl nitriles containing electron-withdrawing or donating substituents. As indicated in Table 4, it is evident that our method is reasonably general and can be applied to several types of aryl nitriles. In all cases the reaction gave the corresponding products in good to excellent yields. The products were

characterized on the basis of their spectral (IR, NMR) and melting points and compared with the literature.^{12–15} The structure of the 5-substituted-1*H*-tetrazoles was in agreement with their spectra data. The disappearance of one strong and sharp absorption band (CN stretching band), and the appearance of an NH stretching band in the IR spectra, were evidence for the formation of tetrazoles (Fig. 7). The carbon of the tetrazole ring can be seen at about $\delta = 150\text{--}157$ ppm in the ¹³C NMR (Fig. 8).¹⁶ The free N–H bond of tetrazoles (NH^T) makes them acidic molecules, and not surprisingly it has been shown that both the aliphatic and aromatic heterocycles have p*K*_a values that are similar to the corresponding carboxylic acids, due to the ability of the moiety to stabilize a negative charge by electron delocalization.¹⁶ In general, tetrazolic acids exhibit physical characteristics similar to

carboxylic acids. Thus, signal of the NH proton of the tetrazole ring (NH^T) shifted downfield (Fig. 9).

Catalyst recyclability

The catalyst recycling is an important step as it reduces the cost of the process. Thus, the recovery and reusability of the GO/ZnO nanocomposite catalyst was examined by applying it to the reaction of sodium azide with 4-methylbenzonitrile under the present reaction conditions. After the first run completed, the catalyst was separated by centrifugation, washed with water and ethanol and dried in a hot air oven at 100 °C for 2 h and employed for the next run of the reaction. The activity of the catalyst in five consecutive runs revealed the practical recyclability of the catalyst (Fig. 10). This reusability demonstrates the

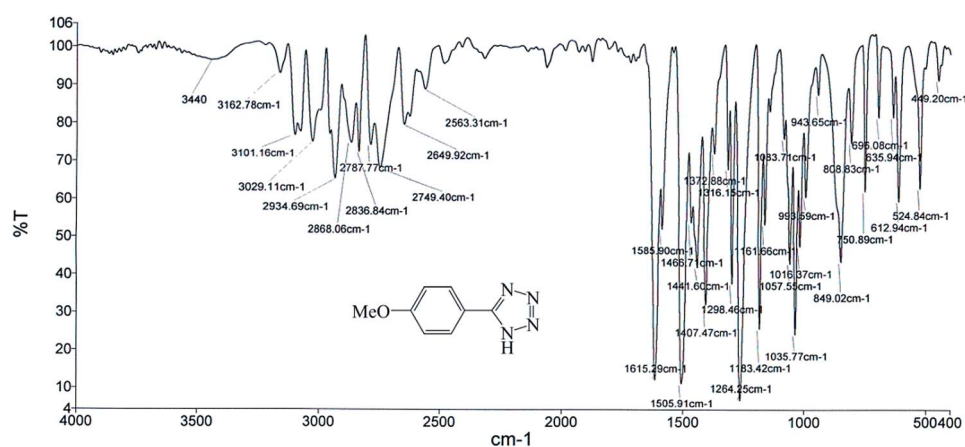


Fig. 7 FT-IR spectrum (KBr) of 5-(4-methoxyphenyl)-1*H*-tetrazole.

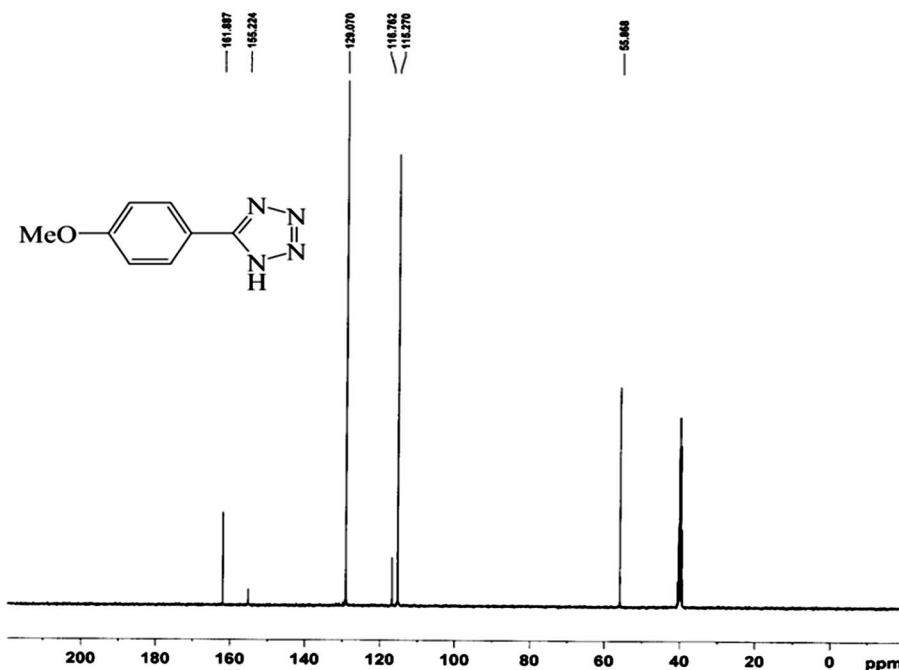


Fig. 8 ¹³C NMR spectrum (100 MHz, DMSO-*d*₆) of 5-(4-methoxyphenyl)-1*H*-tetrazole.

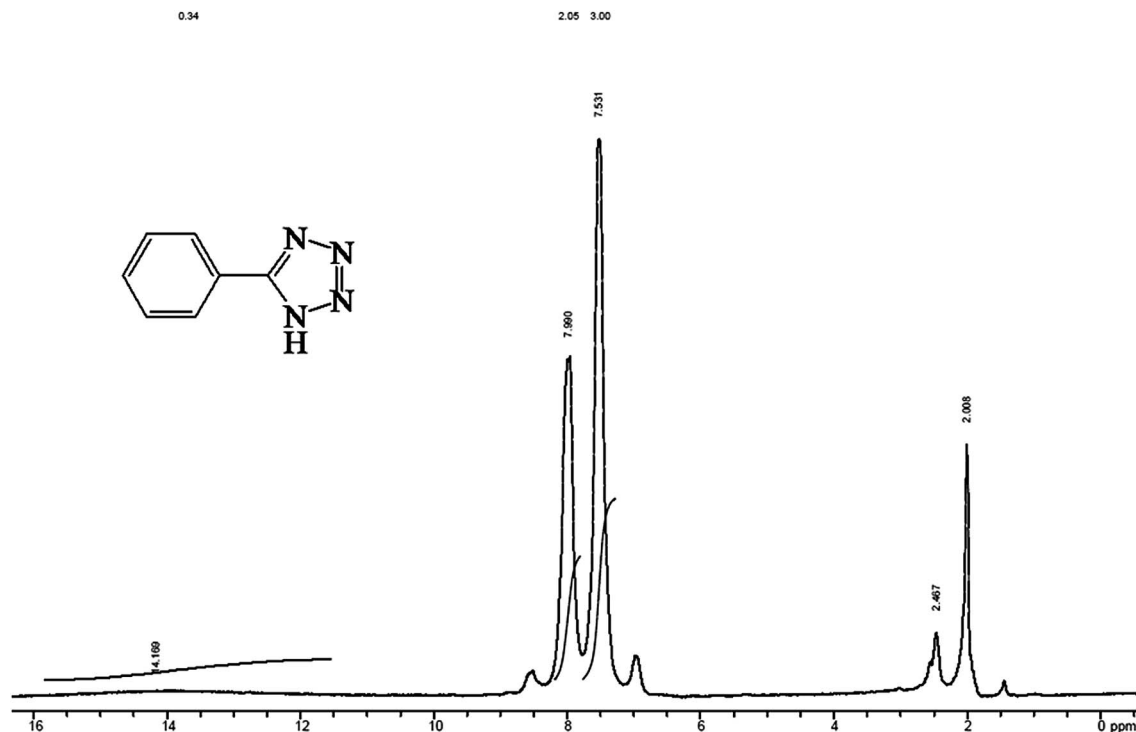


Fig. 9 ^1H NMR spectrum (90 MHz, $\text{DMSO}-d_6$) of 5-phenyl-1H-tetrazole.

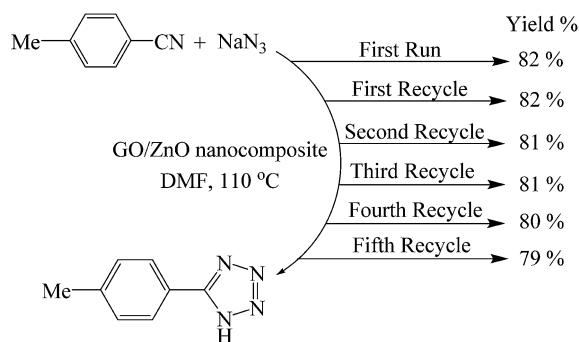


Fig. 10 Reusability of GO/ZnO nanocomposite for the synthesis of 5-(4-methylphenyl)-1H-tetrazole.

high stability and turnover of catalyst under operating condition. The reusability of the catalysts is one of the most important benefits and makes them useful for commercial applications.

Conclusions

In conclusion, we have developed an efficient and simple procedure for preparation of graphene oxide/ZnO nanocomposite as an efficient, easily recoverable and reusable catalyst. The catalyst was characterized by SEM, XRD, EDS, TEM and UV-vis analysis. This catalyst demonstrated a high catalytic activity for synthesis of 5-substituted-1H-tetrazole in high yields. This simple synthetic method has the advantages of high yields, elimination of toxic reagents and expensive, unstable

and homogeneous catalysts, simple methodology and easy work-up. Compared to other catalysts used for similar purposes, GO offers several advantages, including low cost, ease of synthesis, and high stability to ambient conditions. In addition, this methodology offers the competitiveness of recyclability of the catalyst without significant loss of catalytic activity, and the catalyst could be easily recovered and reused for several cycles, thus making this procedure environmentally more acceptable.

Experimental section

All reagents were purchased from the Merck and Aldrich chemical companies and used without further purification. Products were characterized by different spectroscopic methods (FT-IR and ^1H NMR spectra), elemental analysis (CHN) and melting points. ^1H NMR spectra were recorded on a Bruker Avance DRX 90 and 400 MHz instrument. The chemical shifts (δ) are reported in ppm relative to the TMS as internal standard. J values are given in Hz. IR (KBr) spectra were recorded on a Perkin-Elmer 781 spectrophotometer. Melting points were taken in open capillary tubes with a BUCHI 510 melting point apparatus and were uncorrected. The elemental analysis was performed using Heraeus CHN-O-Rapid analyzer. TLC was performed on silica gel polygram SIL G/UV 254 plates. X-ray diffraction measurements were performed with a Philips powder diffractometer type PW 1373 goniometer. It was equipped with a graphite monochromator crystal. The X-ray wavelength was 1.5405 \AA and the diffraction patterns were recorded in the 2θ range (75–15) with scanning speed of 2° min^{-1} . Morphology and particle dispersion was investigated by

scanning electron microscopy (SEM) (Hitachi-Japan-S4160) and transmission electron microscopy (TEM) (Philips CM120). The chemical composition of the prepared catalyst was measured by EDS performed in SEM.

Preparation of graphene oxide (GO)

Graphite oxide was synthesized from commercial graphite by modified Hummers method.¹⁷ The commercial graphite powder (10 g) was put into 230 mL concentrated H₂SO₄ that had been cooled to below of 20 °C with a circulator. Then 30 g potassium permanganate (KMnO₄) was added with stirring, so that the temperature of the mixture was fixed at below of 20 °C. After it, the temperature of the reaction was changed and brought to 40 °C and mixture was stirred at 40 °C for 1 h. Then 500 mL de-ionized water was added to the mixture, causing an increase in temperature to 100 °C. After that 2.5 mL H₂O₂ (30 wt%) was slowly added to the mixture supplementary this solution was diluted by addition 500 L de-ionized water. For purification, the suspension was washed with 1 : 10 HCl solution (200 mL) in order to remove metal ions by filter paper and funnel. The suspension was washed with much de-ionized water at several times, until the filtrate became neutral to remove remaining salt impurities. Exfoliation was performed by sonication for 1 h.

Preparation of graphene oxide/ZnO nanocomposite

GO/ZnO nanocomposite was synthesized with weight ratio of (1 : 1) between GO and ZnO. To synthesize GO/ZnO nanocomposite, 0.5 g dried GO was dispersed in 100 mL of water to form GO suspension by sonication, in which a further exfoliation of GO was achieved. Then, zinc acetate (Zn(CH₃CO₂)₂·2H₂O, 1.1 g) and sodium hydroxide (NaOH, 0.2 g) were successively dissolved slowly in the above GO suspension, followed by sonication for 30 min. Then by using of refluxing method, the mixture stirred at 100 °C for 14 h and after it, cooled to room temperature naturally. Finally, the composite was filtered, washed several times with de-ionized water, and dried at 100 °C for 24 h.

General procedure for the synthesis of 5-substituted-1H-tetrazoles

A mixture of the appropriate nitrile (2.0 mmol), sodium azide (3.0 mmol) and GO/ZnO nanocomposite (0.03 g) was stirred at 120 °C for 30 h. After completion of reaction (as monitored by TLC), the reaction mixture was cooled to room temperature, the catalyst was separated by centrifugation, washed with water and ethanol and the residue was diluted with ethyl acetate (35 mL) and 5 N HCl (20 mL). The resultant organic layer was separated and the aqueous layer was again extracted with ethyl acetate (20 mL). The combined organic layers were washed with water, dried over MgSO₄ and evaporated under reduced pressure using rotary evaporator to give the crude product. The residue was purified by column chromatography to give the desired pure products. The physical and spectral (IR, ¹H NMR and ¹³C NMR) data of the known products were found to be identical with those reported in the literature.^{12–15}

5-Phenyl-1H-tetrazole (Table 2, entry 1). Mp 215–217 °C (lit.¹³ 215–216 °C); ¹H NMR (90 MHz, DMSO): δ_H 7.99–7.53 (m, 5H), 14.17 (s, br, 1H).

5-(4-Methylphenyl)-1H-tetrazole (Table 2, entry 2). Mp 249–251 °C (lit. Aldrich 250–253 °C); ¹H NMR (400 MHz, DMSO): δ_H 7.92 (d, *J* = 7.8 Hz, 2H), 7.40 (d, *J* = 7.8 Hz, 2H), 2.38 (s, 3H); ¹³C NMR (100 MHz, CDCl₃): δ_C 155.6, 141.6, 130.4, 127.3, 121.7, 21.5.

5-(4-Methoxyphenyl)-1H-tetrazole (Table 2, entry 3). Mp 231–233 °C (lit.¹⁴ 231–232 °C); ¹H NMR (400 MHz, DMSO): δ_H 7.97 (d, *J* = 8.6 Hz, 2H), 7.14 (d, *J* = 8.6 Hz, 2H), 3.83 (s, 3H); ¹³C NMR (100 MHz, CDCl₃): δ_C 161.8, 155.2, 129.1, 116.7, 115.3, 55.8.

5-(3-Chlorophenyl)-1H-tetrazole (Table 2, entry 4). Mp 139–141 °C (lit.¹³ 139–140 °C); ¹H NMR (400 MHz, DMSO): δ_H 8.06 (s, 1H), 8.02–7.99 (m, 1H), 7.65 (s, 2H).

5-(4-Chlorophenyl)-1H-tetrazole (Table 2, entry 5). Mp 261–263 °C (lit. Aldrich 260–264 °C); ¹H NMR (400 MHz, DMSO): δ_H 8.07 (d, *J* = 8.4 Hz, 2H), 7.71–7.67 (dd, *J* = 1.6 Hz, *J* = 2.0 Hz, 2H).

5-(4-Fluorophenyl)-1H-tetrazole (Table 2, entry 6). Mp 178–180 °C (lit. Aldrich 180 °C); ¹H NMR (400 MHz, DMSO): δ_H 8.10–8.07 (m, 2H), 7.45–7.40 (m, 2H).

5-(4-Nitrophenyl)-1H-tetrazole (Table 2, entry 7). Mp 220 °C (lit.¹⁴ 220 °C); ¹H NMR (400 MHz, DMSO): δ_H 8.45 (m, 2H), 8.30 (m, 2H).

5-(3-Pyridyl)-1H-tetrazole (Table 2, entry 8). Mp 239–241 °C (lit. Aldrich 238–242 °C); ¹H NMR (400 MHz, DMSO): δ_H 9.20 (s, 1H), 8.59 (s, 1H), 8.34 (d, *J* = 8.0 Hz, 2H), 7.49 (s, br, 1H).

5-(4-Pyridyl)-1H-tetrazole (Table 2, entry 9). Mp 256–258 °C (lit.¹⁵ 255–258 °C); ¹H NMR (400 MHz, DMSO): δ_H 8.75 (s, 2H), 8.01 (d, *J* = 5.6 Hz, 5H), 5.05 (s, br, 1H).

5-(2-Naphthyl)tetrazole (Table 2, entry 10). Mp 206–208 °C (lit.¹⁴ 205–207 °C); ¹H NMR (400 MHz, DMSO): δ_H 8.69 (m, 1H), 8.15 (m, 2H), 8.07 (m, 1H), 8.00 (m, 1H), 7.61 (m, 2H).

5-Benzyl-1H-tetrazole (Table 2, entry 11). Mp 119–121 °C (lit.¹³ 118–120 °C); ¹H NMR (400 MHz, DMSO): δ_H 15.40 (br, 1H), 7.36–7.32 (m, 2H), 7.28–7.24 (m, 3H), 4.30 (s, 2H).

5-(4-Bromophenyl)-1H-tetrazole (Table 2, entry 12). Mp 268–270 °C (lit.¹³ 268–270 °C); ¹H NMR (400 MHz, DMSO): δ_H 16.20 (br, 1H), 8.02–7.99 (m, 2H), 7.86–7.83 (m, 2H).

Acknowledgements

We gratefully acknowledge the Iranian Nano Council and the Universities of Qom and Bu-Ali Sina for the support of this work.

References

- (a) M. Nasrollahzadeh, A. Zahraei, A. Ehsani and M. Khalaj, *RSC Adv.*, 2014, **4**, 20351; (b) H. Shahroosvand, L. Najafi, E. Mohajerani, A. Khabbazi and M. Nasrollahzadeh, *J. Mater. Chem. C*, 2013, **1**, 1337.
- (a) R. J. Herr, *Bioorg. Med. Chem.*, 2002, **10**, 3379; (b) D. Habibi, M. Nasrollahzadeh, L. Mehrabi and S. Mostafaei, *Monatsh. Chem.*, 2013, **144**, 725.
- B. V. LeBlanc and B. S. Jursic, *Synth. Commun.*, 1998, **28**, 3591.

- 4 (a) Y. W. Zhu, S. Murali, M. D. Stoller, K. J. Ganesh, W. W. Cai, P. J. Ferreira, *et al.*, *Science*, 2011, **332**, 1537; (b) M. D. Stoller, S. Park, Y. Zhu, J. An and R. S. Ruoff, *Nano Lett.*, 2008, **8**, 3498.
- 5 D. R. Dreyer, S. Park, C. W. Bielawski and R. S. Ruoff, *Chem. Soc. Rev.*, 2010, **39**, 228.
- 6 B. Seger and P. V. Kamat, *J. Phys. Chem. C*, 2008, **113**, 7990.
- 7 (a) J. Li and C. Y. Liu, *Eur. J. Inorg. Chem.*, 2010, 1244; (b) L. Dong, R. R. S. Gari, Z. Li, M. M. Craig and S. Hou, *Carbon*, 2010, **48**, 781.
- 8 P. Fakhri, B. Jaleh and M. Nasrollahzadeh, *J. Mol. Catal. A: Chem.*, 2014, **383–384**, 17.
- 9 M. Nasrollahzadeh, A. Ehsani and A. Rostami-Vartouni, *Ultrason. Sonochem.*, 2014, **21**, 275.
- 10 (a) L. Tang, Y. Wang, Y. Li, H. Feng, J. Lu and J. Li, *Adv. Funct. Mater.*, 2009, **19**, 2782; (b) M. A. Gondal, Q. A. Drmosh, Z. H. Yamani and T. A. Saleh, *Appl. Surf. Sci.*, 2009, **256**, 298.
- 11 (a) E. Y. Choi, T. H. Han, J. Hong, J. E. Kim, S. H. Lee, H. W. Kim and S. O. Kim, *J. Mater. Chem.*, 2010, **10**, 20; (b) A. Khorsand Zak, W. H. Abd Majid, M. Darroudi and R. Yousefi, *Mater. Lett.*, 2011, **65**, 70.
- 12 M. Nasrollahzadeh, Y. Bayat, D. Habibi and S. Moshaei, *Tetrahedron Lett.*, 2009, **50**, 4435.
- 13 Z. Du, C. Si, Y. Li, Y. Wang and J. Lu, *Int. J. Mol. Sci.*, 2012, **13**, 4696.
- 14 Z. P. Demko and K. B. Sharpless, *J. Org. Chem.*, 2001, **66**, 7945.
- 15 V. Aureggi and G. Sedelmeie, *Angew. Chem., Int. Ed*, 2007, **46**, 8440.
- 16 (a) D. Habibi and M. Nasrollahzadeh, *Monatsh. Chem.*, 2012, **143**, 925; (b) D. Habibi, M. Nasrollahzadeh, H. Sahebkhari and S. M. Sajadi, *Synlett*, 2012, **23**, 2795.
- 17 W. S. Hummers Jr and R. E. Offeman, *J. Am. Chem. Soc.*, 1958, **80**(6), 1339.